

Research Note
23rd International Meshing Roundtable (IMR23)
Optimising Stress Constrained Structural Optimisation

Kristian E. Jensen^a

^a*Imperial College London, London SW7 2AZ, United Kingdom*

Abstract

The community of structural optimisation applies implicit boundary representations on structured meshes for identifying topologies that give rise to stiff and light components. There is a growing interest in multiphysics problems, but the structured meshes constitute an obstacle for resolving the multiple length scales that occur. We demonstrate how a combination of anisotropic mesh adaptation with the most popular optimiser and boundary representation technique can produce mesh independent results for a volume minimisation problem with stress and compliance constraints.

Keywords: topology optimisation ; stress constrained ; anisotropic mesh adaptation

1. Introduction

The problem of numerical discretisation of known geometries is a popular topic in computational geometry, but the software is often used in an iterative manner where it is up to the user to improve the design such that a good geometry can be identified. In contrast, topology optimisation software output the optimal geometry, but this is normally achieved using structured meshes which complicate resolution of multi scale phenomena typical of multiphysics [1].

Anisotropic mesh adaptation is an established technique for ensuring computational efficiency in the context of multiscale problems [2], sometimes reducing the computational work with several orders of magnitude [3].

In contrast, parallelism is the preferred method for speeding up computation within the field of structural optimisation [4]. It is primarily in the context of methods utilising various continuous sensitivities [5,6] that mesh adaptivity has been applied, and even then only in the context of mesh refinement

2. Tools and Setup

We use PRaGMaTic [7] as mesh generator, which employs local mesh modifications to improve a heuristic local mesh quality. The optimal mesh minimises the interpolation error of a variable, and this mesh is defined by a SPD

* Corresponding author. Tel.: +44 (0)2075942921
E-mail address: kristianejlebjerg@gmail.com

matrix field derived from the hessian of said variable [8], the technique is also called the continuous mesh framework. Several metrics can be combined using the inner ellipse method [9].

The problem statement is identical to that of [10], that is 2D linear elasticity, plane stress, in a L-bracket geometry with finite load and support areas, Ω_{load} and $\Omega_{u=0}$, as illustrated in figure 1(a). The minimum compliance problem requires some type of length scale control to be well posed and we opt for a Helmholtz filter [11] to compute a design, $\tilde{\rho}$, with a minimum length scale, L_{min} .

$$\mathbf{0} = \nabla \cdot \underline{\underline{\sigma}}, \quad \underline{\underline{\sigma}} = 2G\underline{\underline{\epsilon}} + \lambda \underline{\underline{I}} \left(\text{Tr}(\underline{\underline{\epsilon}}) + \partial_z u_z \right), \quad \underline{\underline{\sigma}} = \underline{\underline{\sigma}}_{\text{load}} \quad \text{at} \quad \Omega_{\text{load}} \quad \text{and} \quad \mathbf{u} = \mathbf{0} \quad \text{at} \quad \Omega_{u=0} \quad (1)$$

$$\underline{\underline{\epsilon}} = \frac{1}{2} \left(\nabla \mathbf{u} + [\nabla \mathbf{u}]^T \right), \quad \partial_z u_z = -\frac{\nu}{1-\nu} \nabla \cdot \mathbf{u}, \quad G = E \frac{1}{2(1+\nu)}, \quad \lambda = E \frac{\nu}{(1+\nu)(1-2\nu)}, \quad E = E_{\text{max}} \rho^{P_E} \quad (2)$$

$$\tilde{\rho} = \rho + \nabla \cdot L_{\text{min}}^2 \cdot \nabla \tilde{\rho}$$

where \mathbf{u} is the Lagrangian displacement, $\underline{\underline{\sigma}}$ is the stress, $\underline{\underline{\epsilon}}$ is the deformation, $\partial_z u_z$ is the out of plane deformation, $\underline{\underline{I}}$ is the identity tensor, Tr is the trace, G is the shear modulus, λ is Lamé's first parameter, E is Young's modulus, ν is the Poisson ratio, ρ is the design variable bounded between 0 and 1, while P_E is the SIMP penalisation exponent responsible for avoiding intermediate design variables as these contribute little stiffness relative to the amount of material used, when the exponent is equal to 3.

The displacement as well as the design variables are discretised with continuous 1st order polynomials, while we use 2nd order for the filtered design variable, $\tilde{\rho}$. The forward problem defined in equations (1-2) is solved using FEniCS [12].

We use a p-norm for relaxing the local stress constraints to a single global constraint [13]. The idea is that the local constraint is satisfied in the limit of p going to infinity, and with we will show that adaptive meshes allows for $p = 10$, which gives rise to kinks in the design smaller than the minimum length scale. The current design and displacement fields are thus used to calculate the following objective and constraint functions

$$\sigma_{\text{miss}} = E_S \sqrt{\frac{(\epsilon_{11} - \epsilon_{22})^2 + \epsilon_{11}^2 + \epsilon_{22}^2 + 6\epsilon_{12}^2}{2}}, \quad E_S = E_{\text{min}} + (E_{\text{max}} - E_{\text{min}}) \rho^{P_S} \quad (3)$$

$$V = \int_{\Omega} \rho d\Omega, \quad C = \int_{\partial\Omega_{\text{load}}} \mathbf{u} \cdot \underline{\underline{\sigma}}_{\text{load}} \cdot \hat{\mathbf{n}} ds - C_{\text{max}}, \quad S = \left[\int_{\Omega} (\sigma_{\text{miss}} / \sigma_{\text{max}})^p \right]^{1/p} - 1, \quad (4)$$

where C_{max} is the maximum compliance, P_S is the stress penalisation exponent [14], σ_{miss} is the von mises stress and σ_{max} is its maximum value. The discrete gradient of V can be calculated explicitly, and we use dolfint-adjoint [15] to calculate the gradients of S and C . These two discrete gradients are converted to continuous ones by division with the gradient of V and anisotropic Helmholtz smoothing¹ is applied to the stress sensitivity. We apply a Helmholtz filter to the compliance sensitivity, C_{ρ} ,

$$\tilde{C}_{\rho} = C_{\rho} \rho + \nabla \cdot L_{\text{min}}^2 \cdot \nabla \tilde{C}_{\rho}, \quad \hat{C}_{\rho} = \tilde{C}_{\rho} / \rho$$

where \hat{C}_{ρ} is the filtered compliance sensitivity, the use of which corresponds to minimising the compliance of a non-local elasticity problem [16]². These continuous and smooth sensitivities are then used to calculate metrics associated with the compliance and stress constraints. The filtered design variable is used to calculate a metric associated with the volume constraint and all three metrics are combined using the inner ellipse method [9]. After the mesh has been adapted, the optimiser variables are interpolated on to the new mesh. Due to extrapolation at curved boundaries it can become necessary to enforce the box constraints on the asymptotes and design variables after this interpolation step. Once this interpolation step is complete, the continuous sensitivities are converted to discrete ones, and the optimiser is called to update the design variables. We use the method of moving asymptotes [17] as optimiser due to the fact that it is the most popular optimiser in the community of structural optimisation.

¹ This is defined on the continuous level using an equation similar to (2) with a tensor version of L_{min} based on the Steiner ellipse of the elements.

² The filtered design variable is thus only calculated for the purpose of driving the mesh adaptation, it is not used in the interpolation of the Young's modulus

We consider volume minimisation under stress and compliance constraints with a solid initial design, $\rho_0 = 1$.

We make the problem dimensionless using L_{char} and E_{max} as characteristic length scale and pressure, respectively. This is reflected in the set of parameters used in the optimisations, $L_x = L_y = 1.5L_{\text{char}}$, $L_1 = 0.1L_{\text{char}}$, $\underline{\underline{\sigma}}_{\text{load}} = E_{\text{max}}/L_{\text{char}}$, $\nu = 0.3$, $C_{\text{max}} = 2.5E_{\text{max}}L_{\text{char}}^3$, $\sigma_{\text{max}} = 1.5E_{\text{max}}$, $L_{\text{min}} = 5 \cdot 10^{-2}L_{\text{char}}$, $p = 10$, $P_E = 3$, $P_S = 0.5$.

The last four parameters are purely numerical. In addition to these we have scaling factors for the metrics, η , and the c parameter of the MMA optimiser related to enforcement of constraints, which we fix at 10^3 . Finally, we use move limits to limit the design variable change between two iterations to $\Delta\rho$.

3. Results

We calculate mesh metrics corresponding to minimisation of the 2-norm for all mesh metrics. We do not impose a minimum edge length for the elements, nor a maximum edge length or aspect ratio.

In order to investigate mesh independence, we choose the scaling factor related to the metric of the compliance sensitivity as the primary numerical parameter to be varied and scale the number of iteration it_{max} , the move limits and the other scaling factors with a dimensionless version of this, $\eta_{\bar{\rho}}$,

$$it_{\text{max}} = \text{int} \left(600 \sqrt{0.02/\eta_{\bar{\rho}}} \right), \quad \Delta\rho = 0.1 \sqrt{\eta_{\bar{\rho}}/0.02}, \quad \eta_C = \eta_{\bar{\rho}}, \quad \eta_S = 4\eta_{\bar{\rho}},$$

For reference we have performed an optimisation with a large maximum stress ($\sigma_{\text{max}} = 15E_{\text{max}}$), $\eta_{\bar{\rho}} = 0.08$ and a sharp corner to mimic the result of a pure compliance minimization problem. Figure 1(b) thus shows a horizontal bar going to the load, which does not appear in the stress constrained problems presented in the following.

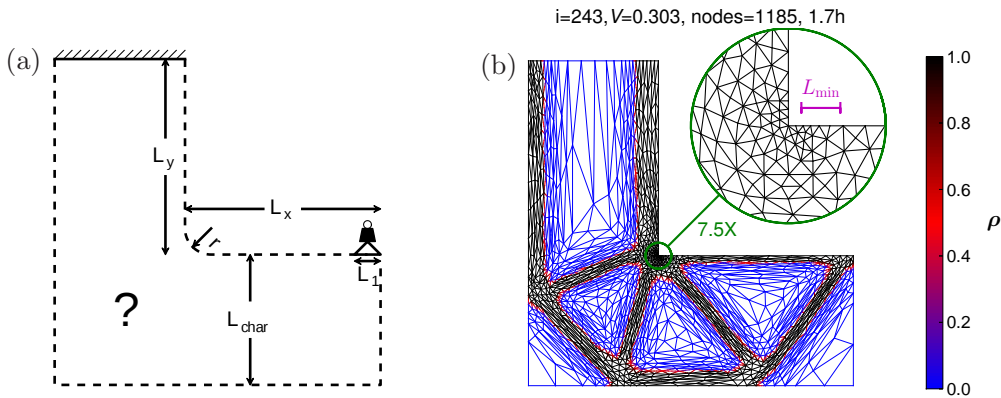


Fig. 1. The L-bracket is a good benchmark for stress constrained topology optimisation due to the stress concentration in the corner of the geometry, (a). The load is distributed over the length L_1 at the tip in order to avoid a stress singularity in the problem definition. Sharp corners can also give rise to stress singularities, and we have investigated the effect of this by rounding the corner. The result of an optimisation using $\sigma_{\text{max}} = 15E_{\text{max}}$ and $\eta_{\bar{\rho}} = 0.08$ is plotted in (b). The large maximum stress results in a design similar to compliance minimisation, thus the bar going horizontally from the load.

We perform optimisations with a sharp ($r = 0$) and a rounded corner ($r = 0.01L_{\text{char}}$) for $\eta_{\bar{\rho}}$ equal to 0.04, 0.02 and 0.01 as shown in figure 2 (a-d). Note that we only show the result for a sharp corner in the case of $\eta_{\bar{\rho}} = 0.02$. We do not expect convergence in a strict sense, so we just plot the design variables and mesh elements for the iteration corresponding to the lowest volume fraction at which the constraints are satisfied to the tolerance of the MMA c parameter. The optimisations with a sharp corner have a component in compression at the load, which might be unstable to perturbations in the load. This behaviour has also been observed in [18], and most likely it can be fixed by using a second load case.

It is well known that structures become weaker as the mesh is refined, i.e. the compliance converges from below and the same is true for the stress. One would thus expect the volume to converge from below in a stress and compliance constrained optimisation problem, but this is not what we see in figure 2(bottom), where the objective function is plotted throughout the optimisations for the sharp as well as the rounded corner. We attribute this convergence

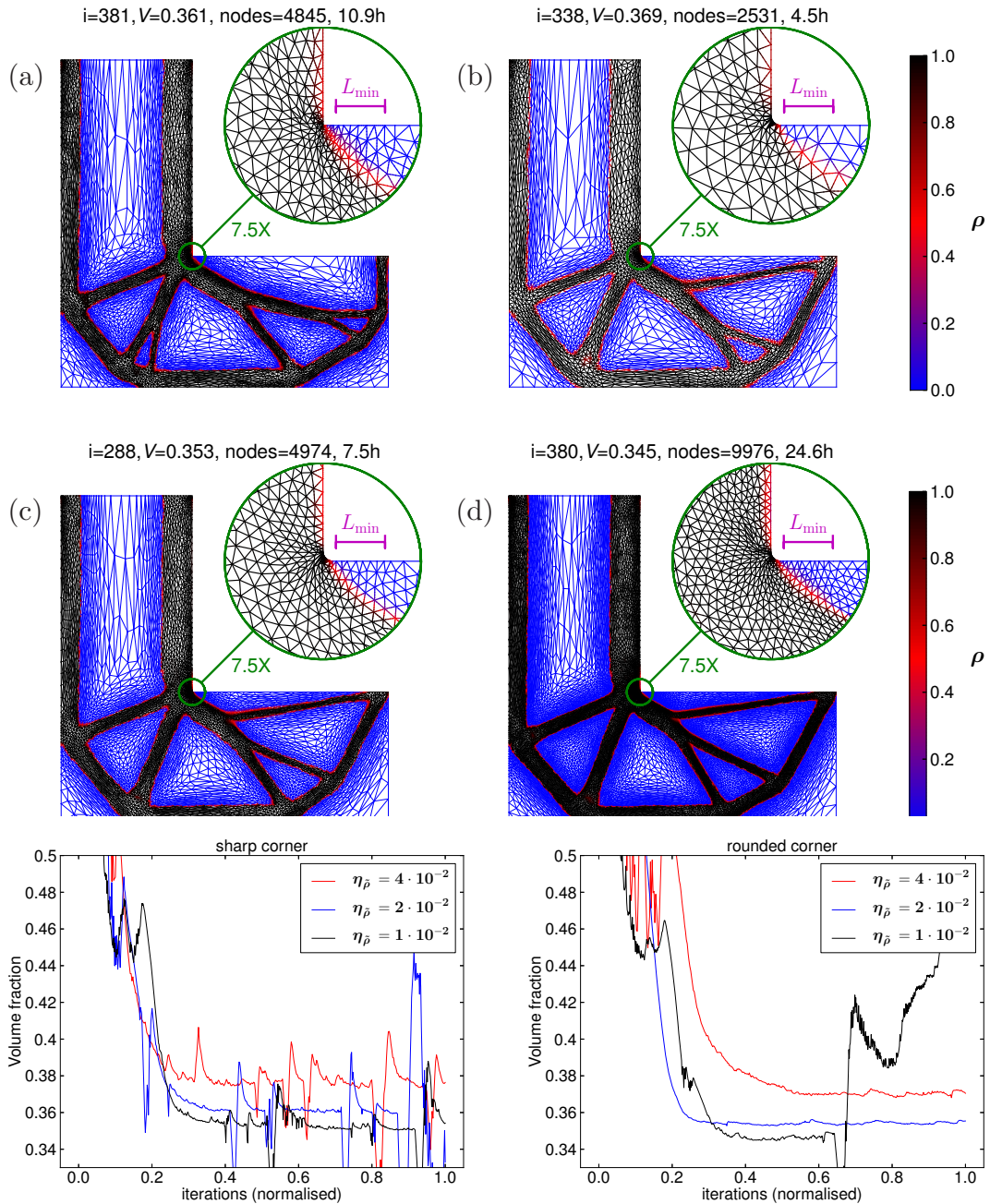


Fig. 2. Optimisations with a sharp (a) and a rounded corner for $\eta_{\bar{\rho}}$ equal to 0.04 (b), 0.02 (a,c) and 0.01 (d). The design variables and mesh elements are shown for the iteration (i) at which the lowest volume fraction (V) occurs, while the stress and compliance constraints are satisfied. The volume fraction is plotted versus normalised iteration numbers for different values of $\eta_{\bar{\rho}}$ in the case of a sharp (left) as well as a rounded corner (right), the latter showing smaller oscillations on the plateaus. The fine optimisation with a rounded corner also show oscillations, but this seems due to issues with infeasible designs.

direction to the sensitivity filter, as this causes the area of intermediate/suboptimal design variables to decrease as the mesh is refined. The plot for the sharp corner has stronger oscillations at the plateaus, possible indicating that the optimiser has an easier time dealing with the rounded corner, which might explain the lack of convergence for the

topology and the objective objective function for the sharp corner. Finally, the plot indicates that the optimisation with $\eta_{\bar{p}} = 0.01$ and a rounded corner falls outside the feasible design space and fails to recover.

4. Conclusion and Future Work

We have performed stress constrained topology optimisations using a combination of anisotropic mesh adaptation and the method of moving asymptotes with interpolation of the asymptotes between iterations. We find that it is necessary to use continuous linear design variables and a sensitivity filter. We argue that it might be beneficial to relax the problem statement to a rounded corner, as a radius of just 1% of the characteristic length scale helps the optimiser find better designs. At least, in this case we are able to demonstrate mesh independence.

In terms of future work it is worth noting, that the meshes occurring during the optimisation loop have only small variations in the later stages of the procedure, meaning that the degrees of freedom are chosen efficiently in the spatial dimension only, not in the "optimisation dimension". We suggest to address this issue using time-space elements and an optimiser defined at the continuous level.

Acknowledgement

This work is supported by the Villum Foundation.

References

- [1] K. Maute, Topology optimization of coupled multi-physics problems, in: *Topology Optimization in Structural and Continuum Mechanics*, Springer, 2014, pp. 421–437.
- [2] M. Piggott, G. Gorman, C. Pain, P. Allison, A. Candy, B. Martin, M. Wells, A new computational framework for multi-scale ocean modelling based on adapting unstructured meshes, *International Journal for Numerical Methods in Fluids* 56 (2008) 1003–1015.
- [3] A. Loseille, A. Dervieux, F. Alauzet, Fully anisotropic goal-oriented mesh adaptation for 3d steady euler equations, *Journal of computational physics* 229 (2010) 2866–2897.
- [4] T. Borrvall, J. Petersson, Large-scale topology optimization in 3d using parallel computing, *Computer methods in applied mechanics and engineering* 190 (2001) 6201–6229.
- [5] M. Wallin, M. Ristinmaa, H. Askfelt, Optimal topologies derived from a phase-field method, *Structural and Multidisciplinary Optimization* 45 (2012) 171–183.
- [6] S. Amstutz, A. A. Novotny, Topological optimization of structures subject to von mises stress constraints, *Structural and Multidisciplinary Optimization* 41 (2010) 407–420.
- [7] G. Rokos, G. J. Gorman, J. Southern, P. H. Kelly, A thread-parallel algorithm for anisotropic mesh adaptation, arXiv preprint arXiv:1308.2480 (2013).
- [8] L. Chen, P. Sun, J. Xu, Optimal anisotropic meshes for minimizing interpolation errors in $\hat{\{}}$ -norm, *Mathematics of Computation* 76 (2007) 179–204.
- [9] C. Baker, A. Buchan, C. Pain, P. Farrell, M. Eaton, P. Warner, Multimesh anisotropic adaptivity for the boltzmann transport equation, *Annals of Nuclear Energy* 53 (2013) 411–426.
- [10] C. Le, J. Norato, T. Bruns, C. Ha, D. Tortorelli, Stress-based topology optimization for continua, *Structural and Multidisciplinary Optimization* 41 (2010) 605–620.
- [11] B. S. Lazarov, O. Sigmund, Filters in topology optimization based on helmholtz-type differential equations, *International Journal for Numerical Methods in Engineering* 86 (2011) 765–781.
- [12] A. Logg, K.-A. Mardal, G. N. Wells, et al., *Automated Solution of Differential Equations by the Finite Element Method*, Springer, 2012. doi:10.1007/978-3-642-23099-8.
- [13] P. Duysinx, O. Sigmund, New developments in handling stress constraints in optimal material distribution, in: *Proc of the 7th AIAA/USAF/NASA/ISSMO Symp on Multidisciplinary Analysis and Optimization*, volume 1, 1998, pp. 1501–1509.
- [14] G. Cheng, X. Guo, ε -relaxed approach in structural topology optimization, *Structural Optimization* 13 (1997) 258–266.
- [15] P. E. Farrell, D. A. Ham, S. W. Funke, M. E. Rognes, Automated derivation of the adjoint of high-level transient finite element programs, *SIAM Journal on Scientific Computing* 35 (2013) C369–C393.
- [16] O. Sigmund, K. Maute, Sensitivity filtering from a continuum mechanics perspective, *Structural and Multidisciplinary Optimization* 46 (2012) 471–475.
- [17] K. Svanberg, The method of moving asymptotes a new method for structural optimization, *International journal for numerical methods in engineering* 24 (1987) 359–373.
- [18] K. Suresh, M. Takaloozadeh, Stress-constrained topology optimization: a topological level-set approach, *Structural and Multidisciplinary Optimization* 48 (2013) 295–309.